Cell J
Cell Journal (Yakhteh)
Archive of SID
Homepage: https://www.celljournal.org/
Original Article
Vol 25, No 3, March 2023, Pages: 194-202

Anticancer Effect of Fluorouracil and Gum-Based Cerium Oxide Nanoparticles on Human Malignant Colon Carcinoma Cell Line ($Caco_2$)

Zahra Keramati, M.Sc.[1], Gholamreza Motalleb, Ph.D.[1*], Abbas Rahdar, Ph.D.[2], Mohammad Amin Kerachian, Ph.D.[3]

1. Division of Cell and Molecular Biology, Department of Biology, Faculty of Science, University of Zabol, Zabol, Iran
2. Department of Physics, Faculty of Science, University of Zabol, Zabol, Iran
3. Department of Medical Genetics, Faculty of Medicine, Mashhad University of Medical Sciences, Mashhad, Iran

Abstract

Objective: We investigated whether co-incubation of 5-FU and gum-based cerium oxide nanoparticles (CeO_2 NPs) would improve half-maximal inhibitory concentration (IC_{50}) and apoptosis in the Caco-2 cancer cell line

Materials and Methods: In this experimental study, we synthesized Ceo-2-XG by the nano perception method. X-ray diffraction (XRD), field emission scanning electron microscopy (FESEM), transmission electron microscopy (TEM), dynamic light scattering (DLS) and vibrating sample magnetometer (VSM) techniques were employed to characterize the synthesized nanoparticles. The Caco-2 cancer cells were cultured and treated with Ceo-2-XG and 5-FU. Cytotoxicity analysis was carried out using MTT assay on Caco-2 cancer cells. *CXCR1, CXCR2, CXCL8, BAX, BCL-2, P53, CASPASE-3, CASPASE-8* and *CASPASE-9* gene expression changes were assessed by quantitative reverse-transcriptase polymerase chain reaction (qRT-PCR). The Caco-2 cancer cell mortality mechanism was analyzed using Annexin V-FITC/PI flow cytometry. Using the inverted microscope morphology changes of the Caco-2 cancer cells was observed.

Results: With a sample size of roughly 11 nm, TEM analysis revealed spherical structures. Interestingly, after 72 hours, 400 µg/ml nanoparticles significantly lowered the IC_{50} of 5-FU from 101 to 71 µg/ml (P<000.1). Furthermore, qRT-PCR analysis showed that *BCL-2, CXCR1, CXCR2* and *CXCR8* expressions were significantly decreased in the 5-FU and Ceo-2-XG nanoparticles co-incubated group, compared to the 5-FU alone (P<0.001). Notably, gene expressions of *BAX, P53, CASPASE-3, CASPASE-8* and CASPASE-9 were significantly higher in the 5-FU and Ceo-2-XG nanoparticles co-incubated group, compared to the 5-FU alone (P<0.001). The findings revealed that dead cells owing to apoptosis were more than two times higher in 5-FU and Ceo-2-XG nanoparticles cancer cells than in 5-FU alone treated cancer cells.

Conclusion: Co-incubation of 5-FU and Ceo-2-XG nanoparticles significantly increased apoptosis in the Caco-2 cancer cells. The antiproliferative activity of co-incubated 5-FU and Ceo-2-XG nanoparticles on Caco-2 cancer cells was substantially higher than that of 5-FU alone.

Keywords: Apoptosis, Caspases, Colorectal Neoplasms, Oncogenes

Citation: **Keramati Z, Motalleb Gh, Rahdar A, Kerachian MA. Anticancer effect of fluorouracil and gum-based cerium oxide nanoparticles on human malignant colon carcinoma cell line ($Caco_2$). Cell J. 2023; 25(3): 194-202. doi: 10.22074/CELLJ.2023.562683.1135.**

Introduction

Thirteen million cancer deaths and more than 21 million new cancer cases are predicted by 2030 (1). In 2020, there were about 2 million new colorectal cancer (CRC) diagnoses with over 900,000 deaths (2). CRC encompasses high genetic heterogeneity and hard-to-establish unique mutations. Deficit of genomic stability, such as aberrant DNA-methylation, chromosomal instability and microsatellite instability, leads to CRC development by gaining novel mutations related to tumor phenotype (3). 5-FU is an antimetabolite drug that has been extensively employed to cure CRC and breast cancer. Although 5-FU has the uppermost effect in the therapy of developed CRC, the response rate is only 10-15%. Therefore, new treatment plans are needed as soon as possible to fight drug resistance and increase the drug response rate. Nanoparticles play a significant role in many areas of physics, chemistry and material sciences (4). Cerium oxide nanoparticles (CeO_2 NPs) or nanoceria has been significantly used in biomedical research due to their free-radical scavengers, radioactivity protection, drug distribution and delivery, cancer biomarker and anti-inflammatory characteristics (5). Co-cultures and nano organic culture system applications have been routinely developed in toxicology, drug delivery science and technology.

Received: 26/September/2022, 24/December/2022, Accepted: 08/January/2023
***Corresponding Address: P.O.Box: 98613-35856, Division of Cell and Molecular Biology, Department of Biology, Faculty of Science, University of Zabol, Zabol, Iran**
Email: reza.motaleb@uoz.ac.ir

Royan Institute
Cell Journal (Yakhteh)

Apoptosis is usually indicated with different structural changes and energy-dependent biochemical mechanisms. Many processes, including normal cell proliferation, immune system growth and activity, hormone-dependent atrophy, embryonic growth and chemically induced cell death, are thought to depend on apoptosis. Incorrect apoptosis, either too slight or too abundant, is an issue in different kinds of cancer. So, investigation emphasizes clarifying and examining the cell cycle system with signaling pathways that operate apoptosis. Apoptosis is a kind of "programmed" cell death that influences genetically specified removal of cells. One of the most important genes in apoptosis is *P53*. The p53-induced apoptosis induces DNA repair early, which it may be needed to reverse cell death. Apoptosis is a coordinated, energy-dependent procedure that starts a cascade of cysteine proteases, leading to cell death. Caspases-3, the most important effector caspase, is triggered by caspase-8 and caspase-9. *BCL-2* family has 25 genes. Anti-opoptotic proteins include Bcl-2, Bcl-x, Bcl-XL, Bcl-XS, Bcl-w and BAG. Pro-opoptotic proteins include Bcl-10, Bax, Bid, Bad, Bim, Bik and Blk. These proteins determine whether a cell must undergo apoptosis or not (6). Numerous reports proposed that CXCs proteins arbitrated several phases throughout angiogenesis. The recent studies confirmed that CXCL8 (belong to ELR+CXC chemokine family) and its receptors, CXCR1 and CXCR2, are powerful angiogenic regulators. Many cancers and endothelial cells expressed CXCR1 and CXCR2 (7). In this research project, we intended to upsurge and improve the anticancer effect of 5-FU using CeO_2 NPs based on green synthesis with xanthan gum (Ceo-2-XG) in a co-incubation cancer model to develop a novel, less invasive and 5-FU nano-delivery method on the human malignant colon carcinoma cells (Caco-2). The core of our preliminary *in vitro* evaluation is based on IC50 values. The present study also intended to offer a proof-of-concept on the mechanism of *CXCR1, CXCR2, CXCL8, BAX, BCL-2, P53, CASPASE-3, CASPASE-8,* and *CASPASE-9* gene expressions and activities in the apoptotic pathway after treatment of Caco-2 by 5-FU and Ceo-2-XG.

Materials and Methods

Ce $(NO_3)3.6H_2O$ (Sigma-Aldrich, USA), C35H49O29 (Sigma-Aldrich, USA), NaOH (Sigma-Aldrich, USA), EDTA (Merck, Germany), Agarose (Fermentas, UK), Tris base (Merck, Germany), Green viewer (SinaClon, Iran), Loading dye buffer (6X; SinaClon, Iran), Fetal Bovine Serum (Gibco, Canada), DMEM-high Glucose (Gibco, Canada), Gentamicin (Gibco, Canada), Triton X-100 (Merck, Germany), 5-FU (Cayman Thermo Fisher Scientific, USA), MTT powder (Auto Thermo Fisher Scientific, USA), PI (MabTag GmbH, Germany), Annexin (MabTag GmbH, Germany), Penicillin and Streptomycin (Biosera, USA), DMSO (Merck, Germany), Trypsin (Gibco, Canada).

This research was approved by University of Zabol with Ethics committee letter number MAA-131.

Culture of cells

The human malignant colon cancer cell line (Caco-2) was purchased from Pasteur Institute (Tehran, Iran). The cells were grown in Dulbecco's Modified Eagle's Medium (DMEM), High glucose) (Gibco, Canada) containing 10% fetal bovine serum (FBS) with 0.2% Gentamicin at 37°C under 5% CO_2, 95% air and 70-80% humidity environment.

Preparation of 5-FU and Ceo-2-XG

5-FU (250 mg/ml) was purchased from Cayman Thermo Fisher Scientific, USA. The Ceo-2-XG nanoparticles were made using the technique reported before (8). In brief, co-precipitation was used to create Xanthan Gum-stabilized Cerium oxide nanoparticles (CeNPs) using cerium nitrate $[Ce(NO_3)3.6H_2O]$ as a primary precursor and Xanthan gum ($C_{35}H_{49}O_{29}$) and a green stabilizing agent. X-ray diffraction, field emission scanning electron microscopy, transmission electron microscopy (TEM), dynamic light scattering (DLS) and vibrating sample magnetometer methods were used to characterize the synthesized nanoparticles. All procedures were done at room temperature. The final product was kept for further tests. Figure 1 depicts the schematic of the nanoparticles made and employed in this investigation.

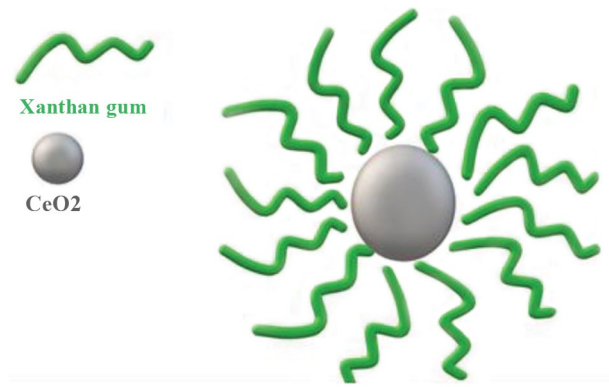

Fig.1: Schematic Ceo-2-XG nanoparticles.

Techniques for characterization

D8 Advance X'Pert X-Ray diffractometer (Bruker, Germany) was used to perform powder diffraction on Ceo-2-XG nanoparticles microstructure. TEM analysis was carried out using Zeiss SUPRA 55-VP FEGSEM (Zeiss, Germany). Surface morphology and nanoparticles size were studied by FESEM (Tescan, Czech Republic). To demonstrate size, DLS (Malvern Instruments, UK) technique with a HeNe laser source (633 nm) was used. The Kavir Precise Magnetic instrument (MDKFT, Iran) was used to perform a vibrating sample magnetometer (VSM) (8). The made Ceo-2-XG nanoparticles were kept for one week to examine aggregation and electron microscopy. In this study, the fundamental concept of our initial *in vitro* assessment is based on half-maximal inhibitory concentration (IC_{50}) values (9).

MTT test

Caco-2 cancer cells were cultivated and maintained

for 72 hours using 5-FU and Ceo-2-XG nanoparticles. Cytotoxicity of free 5-FU (1, 5, 10, 20, 40, 60, 80, 100, 200, 300 and 400 µg/ml), Ceo-2-XG (10, 20, 40, 60, 80, 100, 200, 300, 400, 500, 600, 700 and 800 µg/ml), 5-Fu (100 µg/ml) with Ceo-2-XG (10, 20, 40, 60, 80, 100, 200, 300, 400, 500, 600, 700, 800 and 1000 µg/ml), Ceo-2-XG (400 µg/ml) with 5-Fu (1, 5, 10, 20, 40, 60, 80, 100, 200, 300 and 400 µg/ml) were carried out using (3-(4,5-dimethylthiazol-2-yl)-2,5-diphenyl tetrazolium bromide; MTT) assay on Caco-2 cancer cells (10). Briefly, the cells were seeded at 1×10^5 per well on 96-well plates, cultivated for 24-72 hours and subsequently tested for cytotoxicity by different doses of 5-FU and Ceo-2-XG nanoparticles using MTT assay. The MTT (0.5 mg/ml) reagent was then applied to the wells. The well plates were then incubated at 37°C in 5% CO_2 for four hours. After dissolving the crystals in DMSO, the absorbance at 570 nm was measured using an Epon microplate reader (BioTek, USA) and well cells as blanks. The percentage survival rate of cells was calculated using the following formula (11):

$$\text{The survival rate in percentage} = \frac{\text{Absorb treated well (570 nm) - Absorb blank well (570 nm)}/\text{Absorb conrol well (570 nm)}}{\text{Absorb treated well (630 nm) - Absorb blank well (630 nm)}/\text{Absorb conrol well (630 nm)}} \times 100$$

IC_{50} values were calculated and analyzed using GraphPad Prism software version 8 (GraphPad, USA) (12).

RNA isolation and synthesis of cDNA

Using the Parstous Total RNA Extraction kit (Parstous Biotech, Iran), total RNA extraction and cDNA synthesis were carried out in accordance with the manufacturer's guidelines. Electrophoresis was used to assess the quality of the extracted RNA.

Real-time quantitative reverse transcription polymerase chain reaction

CXCR1, *CXCR2*, *CXCL8*, *BAX*, *BCL-2*, *P53*, *CASPASE-3*, *CASPASE-8* and *CASPASE-9* expression changes were analyzed using the Parstous 2X SYBR Green Real-Time PCR Kit (Parstous Biotech., Iran). The synthesized cDNA was exposed to primers for SYBER green real-time polymerase chain reaction (PCR). The housekeeping gene was glyceraldehyde-3-phosphate dehydrogenase (*GAPDH*). Table S1 (See Supplementary Online Information at www.celljournal.org) displays the quantitative reverse transcription PCR (qRT-PCR) conditions. The $2^{-\Delta\Delta Ct}$ method was used to quantify genes expression (13). The Primer3 package created all primers automatically (14). Then, primer specificity was predicted further, using the online program Primer-Blast (15).

Apoptosis assessment by flow cytometry

Mechanism of Caco-2 cancer cell death, produced by 5-FU and Ceo-2-XG nanoparticles, was studied using Annexin V-FITC/PI flow cytometry (16). In brief, 5×10^5 cancer cells were cultivated in each well plate using 2 ml of medium (DMEM-high glucose). When the cells attained an 80 percent density, they were given an effective dosage of 5-FU and 5-FU plus Ceo-2-XG nanoparticles. Then, in turn, the following painting stages were carried out: each well was treated with trypsin and rinsed with phosphate-buffered saline (PBS). For five minutes, centrifugation was done at 400 rpm. The supernatant was discarded. The precipitate was then dissolved in 200 µl of Annexin-Binding buffer. Centrifugation was repeated at 400 rpm for five minutes. The supernatant was thrown away. After that, the precipitate was dissolved in 50 µl of annexin V-FITC/PI solution and incubated for 10 minutes at room temperatureat in the dark. 150 µl Annexin-binding buffer was added. Finally, the BD FACSCaliburTM Flow Cytometer (BD Biosciences, Canada) system was used to read the samples. The findings were analyzed using FlowJo software version 10 (BD, USA).

Light microscopy

An inverted microscope was used to see how the shape of cancer cells changed after they were treated with 5-FU and Ceo-2-XG nanoparticles (Labomed TCM 400, USA) (17).

Statistical evaluation

The whole data set was examined using the SPSS program (SPSS Inc., USA), version 21, which was reported as a mean standard deviation. Each assessment was performed three times separately. The two-way analysis of variance (two-way ANOVA) with Tukey post-test were used to evaluate numerous groups. $P<0.001$ was regarded as highly statistically significant.

Results

The goal of this study was to increase the anticancer impact of 5-FU using xanthan gum-based cerium oxide nanoparticles (Ceo-2-XG) on the malignant human colon carcinoma cell line (Caco-2).

5-FU and Ceo-2-XG nanoparticle characterizations

Low-energy spontaneous emulsification was used to create the 5-FU and Ceo-2-XG nanoparticles microemulsions. After one week of preparation, visual stability of the 5-FU and Ceo-2-XG microemulsions was established. There was no evidence of aggregation. Morphology of Ceo-2-XG nanoparticles was then examined using FESEM. Ceo-2-XG nanoparticles were spherical, with a sample size of around 20nm, as illustrated in Figure 2A, B and C. Figure 2D demonstrates XRD pattern for nanometer-sized cerium oxide particles calcined at various temperatures (200, 400, 600 and 800°C). Crystalline structure of the nanocrystals was established using the X-ray diffraction (XRD) method. Findings match the crystallographic reference data (JCPDS # 01-075-0076). Lack of the extra peaks in the diffraction patterns verified the compound's excellent purity. Comparison of diffraction

patterns is shown in Figure 2D. As it can be observed, raising the content of plant extract from 10 to 30 ml widens the peaks and lowers crystallization, suggesting smaller nanoparticles.

Impact of 5-FU and Ceo-2-XG nanoparticles on Caco-2 cancer cell growth suppression and viability

Findings showed that IC_{50} for 5-FU was 101 µg/ml, as shown in Figure 3A. As demonstrated in Figure 3B, the synthesized Ceo-2-XG nanoparticles did not exhibit substantial toxicity even at 1000 µg/ml (toxicity rate was more than 50%). Because Ceo-2-XG nanoparticles are non-toxic to Caco2 cancer cells, an effective nanoparticle dose that may aid in increasing the permeability of 5-FU was found in two phases. First, we looked at the cytotoxicity of 5-FU at a constant dosage of 100 µg/ml with different nanoparticle concentrations (10-1000 µg/ml). Figure 3C shows that 5-FU (101 µg/ml) reduced IC50 of Ceo-2-XG nanoparticles to 400 µl/ml. In the second scenario, we tested cytotoxicity of Ceo-2-XG nanoparticles with varied quantities of 5-FU (1-400 µg/ml) for 72 hours at a constant concentration of 400 µg/ml. Surprisingly, 400 µg/ml of Ceo-2-XG nanoparticles reduced IC50 of the 5-FU from 100 µg/ml to 71 µg/ml, as illustrated in Figure 3D.

Quantitative reverse transcription polymerase chain reaction

Gene expression alterations in *CXCR1*, *CXCR2*, *CXCL8*, *BAX*, *BCL-2*, *P53*, *CASPASE-3*, *CASPASE-8*, and *CASPASE-9* were assessed by qRT-PCR, as shown in Figure 4. Findings indicated that *BCL-2*, *CXCR1*, *CXCR2* and *CXCL8* gene expressions were reduced in the 5-FU treated cancer cells compared to the untreated cancer cells (P<0.001). However, gene expressions of *BAX*, *P53*, *CASPASE-3*, *CASPASE-8*, and *CASPASE-9* were elevated (P<0.001). Significantly, gene expressions of *BCL-2*, *CXCR1*, *CXCR2* and *CXCL8* were reduced in the 5-FU and Ceo-2-XG nanoparticles co-incubated treated cancer cells group compared to the untreated cancer cells, as the control group (P<0.001). Gene expressions of *BAX*, *P53*, *CASPASE-3*, *CASPASE-8*, and *CASPASE-9* were higher in the 5-FU and Ceo-2-XG nanoparticles co-incubated treated cancer cells compared to the untreated cancer cells (P<0.001). In the second scenario, we compared the gene expressions in cancer cells treated with 5-FU alone (as the control group) to those treated with 5-FU and Ceo-2-XG nanoparticles co-incubated. Interestingly, gene expressions of *BCL-2*, *CXCR1*, *CXCR2* and *CXCL8* were considerably lowered in the cancer cells co-incubated treated with 5-FU and Ceo-2-XG nanoparticles than in the cancer cells treated with 5-FU alone (P<0.001). Notably, gene expression of *BAX*, *P53*, *CASPASE-3*, *CASPASE-8* and *CASPASE-9* was considerably higher in the 5-FU and Ceo-2-XG nanoparticles co-incubated treated group compared to cancer cells treated with 5-FU alone (P<0.001).

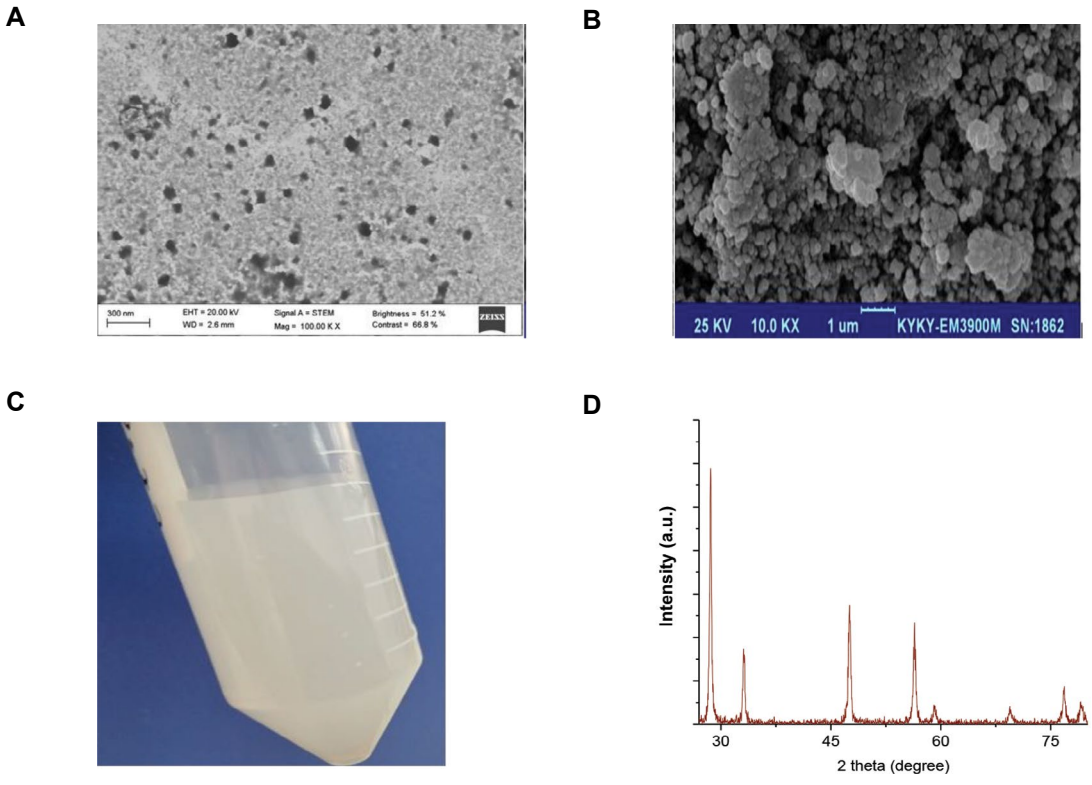

Fig.2: Morphology analysis of Ceo-2-XG nanoparticles and XRD analysis. **A.** TEM (magnification: 1,000,000x). **B.** FESEM of Ceo-2-XG nanoparticles, nanoparticles were spherical, with a sample size of roughly 20 nm (magnification: 700,000x). **C.** Ceo-2-XG nanoparticles dispersed in PBS. No aggregation was observed. **D.** X-ray diffraction pattern of Ceo-2-XG nanoparticles. XRD; X-ray diffraction, TEM; Transmission electron microscopy, FESEM; Field emission scanning electron microscopy, and PBS; Phosphate-buffered saline.

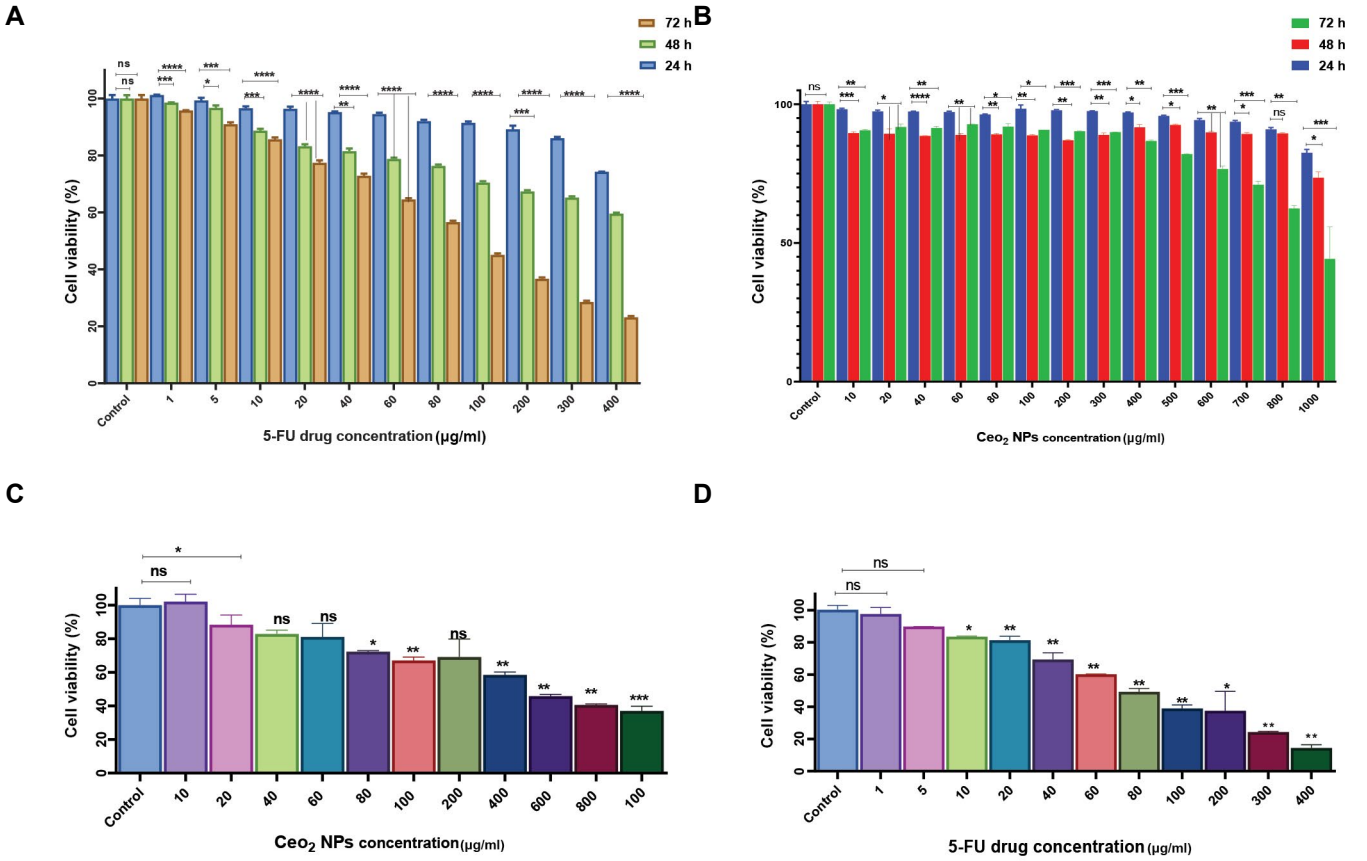

Fig.3: Cytotoxicity of 5-FU and Ceo-2-XG nanoparticles at varied doses on $Caco_2$ cancer cells. **A.** $Caco_2$ cancer cells viability percentage treated with 5-FU drug (P<0.001). **B.** $Caco_2$ cancer cells viability percentage treated with the synthesized Ceo-2-XG nanoparticles for 24, 48, 72 hours (P<0.001). **C.** Viability percentage of $Caco_2$ cancer cells treated with various concentrations of Ceo-2-XG nanoparticles in the presence of a constant quantity of 5-FU (100 µg/ml) in a co-cultured model (P<0.001). **D.** Viability percentage of $Caco_2$ cancer cells treated with various concentrations of 5-FU (1-400 µg/ml) in the presence of a constant concentration of Ceo-2-XG nanoparticles (400 µg/ml) in a co-incubated model (P<0.001). ns; P≥0.06, *; 0.01≤P≤0.05, **; 0.00≤ P≤0.009, ***; 0.0004≤P≤ 0.0009, and ****; 0.0000≤P≤0.0004, and h; Hour.

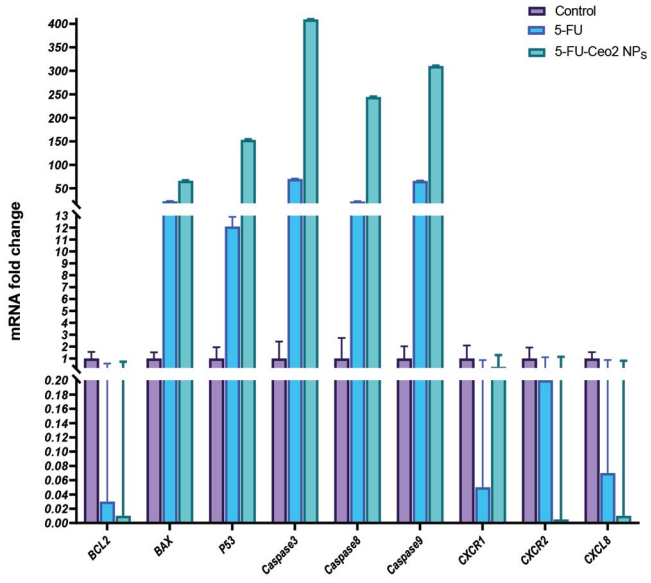

Fig.4: Changes in the expression of *BCL2* (P=0.00), *BAX* (P=0.00), *P53* (P=0.00), *CASPASE-3* (P=0.00), *CASPASE-8* (P=0.00), *CASPASE-9* (P=0.00), *CXCR1* (P=0.00), *CXCR2* (P=0.00) and *CXCL8* (P=0.00, P<0.001).

Flow cytometry for apoptosis evaluation

Mortality of Caco-2 cancer cells caused by apoptosis, due to induction of co-incubated 5-FU and Ceo-2-XG nanoparticles was studied using Annexin V-FITC/PI flow cytometry. Interestingly, findings revealed that dead cells owing to apoptosis were 35.96%, which was more than two times higher in the 5-FU and Ceo-2-XG nanoparticles co-incubated treated cancer cells than in the 5-FU alone treated cancer cells (17.14%; Fig.5A-D). On the other hand, compared to the untreated cancer cells in the control group, percentage of dead cells in the 5-FU plus Ceo-2-XG nanoparticles and the 5-FU alone treated cancer cells was more than 27 and 13 times higher, respectively. Early apoptotic cells in the 5-FU and Ceo-2-XG nanoparticles were more than five times greater than in 5-FU alone treated cancer cells. Early apoptotic cells in the 5-FU and Ceo-2-XG nanoparticles, on the other hand, were more than

41 times more than the untreated cancer cells in the control group.

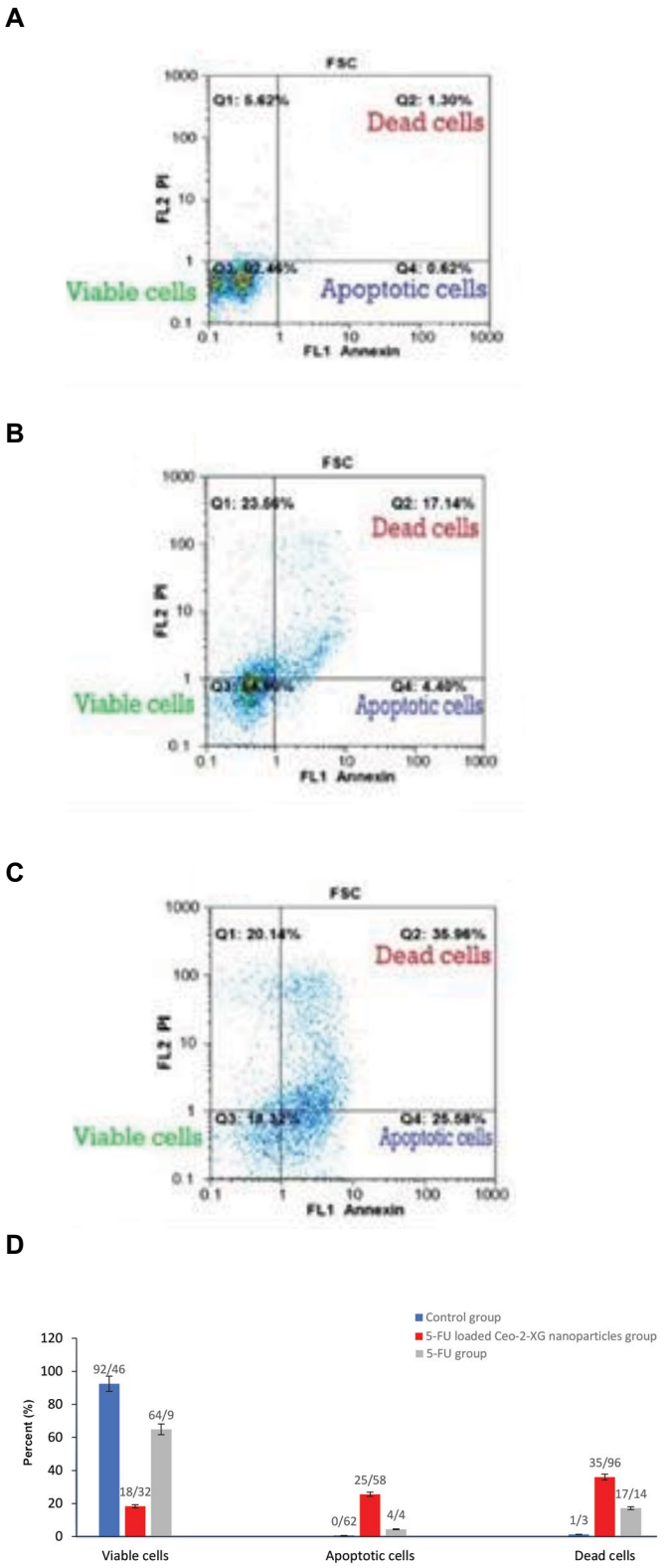

Fig.5: Flow cytometry of treated Caco2 cancer cells during 72 hours. Identified apoptotic cells based on Annexin V-FITC/PI staining. **A.** No treated Caco2 cancer cells group (control group). **B.** 5-FU treated Caco2 cancer cells. **C.** Co-cultured 5-FU and Ceo-2-XG nanoparticles treated group (P<0.001). **D.** Scatter diagram of flow cytometry (P<0.001).

Inverted light microscopy

Morphological alterations in the Caco-2 cancer cells after 72 hours of co-incubation with 5-FU and Ceo-2-XG nanoparticles are illustrated in Figure 6A-C. The cells began to round and lose their shape. With increased concentration, these changes intensified and many cells separated to form irregularly shaped masses. At greater dosages, cell density was dropped as well.

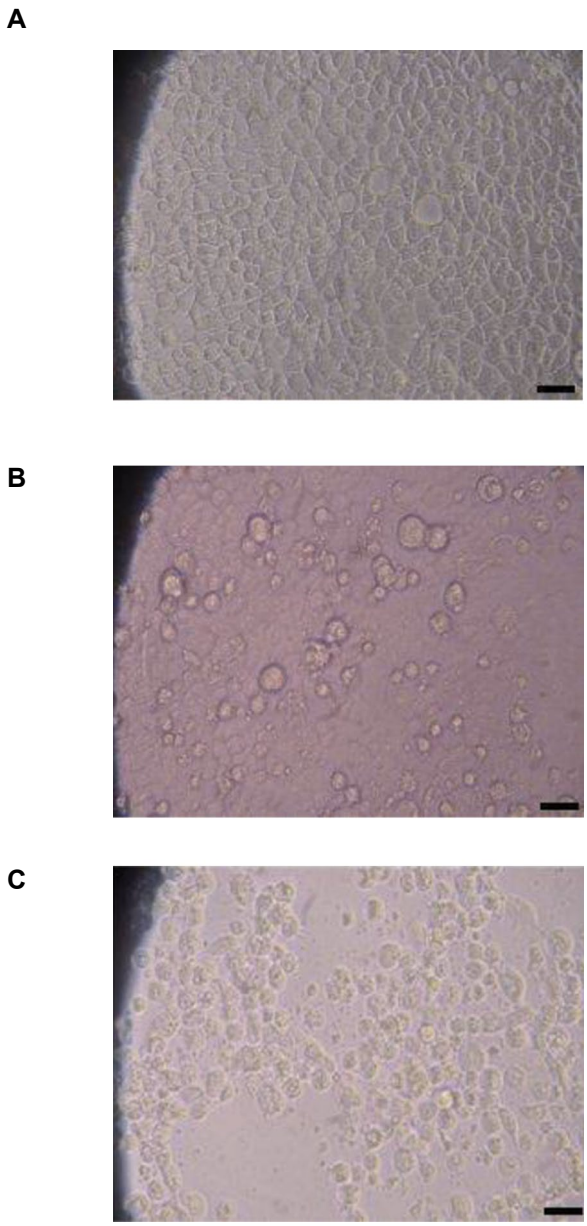

Fig.6: Light micrographs of the cancer cell treated groups. **A.** Cancer cells untreated group (control group). **B.** 5-FU treated cancer cells group, and **C.** 5-FU and Ceo-2-XG nanoparticles co-incubated treated cancer cells group (scale bar: 20 µm, magnification: 20x).

Discussion

This work aimed to increase antineoplastic impact of 5-FU upon malignant Caco-2 cancer cells in a co-incubated model using xanthan gum-based

cerium oxide nanoparticles (Ceo-2-XG). The major important result was that co-incubated 5-FU and Ceo-2-XG nanoparticles with Caco-2 cancer cells considerably induced more apoptosis than the 5-FU alone in a dose and time dependent manner. Radiation, chemotherapy, surgery, nutritional supplement treatment, and immunotherapy may cure CRC, however their adverse effects reduce their success rates.

Though 5-FU inhibits DNA synthesis, its therapeutic efficacy is diminished owing to its hydrophilic nature and rapid breakdown by dihydropyrimidine dehydrogenase. A high dosage of 5-FU causes severe gastrointestinal and neurological side-effects (18). Therefore, enhancing and inventing a creative distribution system is critical in order to safeguard and deliver a magnificent cargo of 5-FU to the desired location with more healing efficacy.

Nanotechnology has paved the way for developing innovative and effective nanomaterials in CRC treatment (19). Nano-emulsions, Cerium Oxide (CeO_2), quantum dots, gold NPs, liposomes, silica NPs and dendrimers are examples of nano-formulations under development (20). The biogenic CeO_2 NPs demonstrated excellent anticancer properties (21). In this regard, xanthan gum is an anionic polysaccharide produced naturally by several Xanthomonas bacteria (22).

Biogenic culture methods have been increasingly common in toxicology because of the growing requirement for more extensive *in vitro* examinations which can better simulate the *in vivo* condition, particularly for the poisonousness evaluation of cumulative NPs (23).

Visual stability of the 5-FU and Ceo-2-XG microemulsions was assessed after one week of preparation in this study. There was no indication of aggregation. According to SEM, Ceo-2-XG nanoparticles were spherical, with a sample size of roughly 20 nm. Variety of vascular apertures of tumors is 10-1000 nm and NPs smaller than 10 nm will accumulate in the kidney, liver, spleen and lymph nodes. On the other hand, NPs bigger than 100 nm are eliminated from lung (24). Thus, our findings showed that Ceo-2-XG nanoparticles improved efficacy and 5-FU drug delivery in the co-incubation scenario of the Ceco-2 cancer cells. Average hydrodynamic diameters of Ceo-2-XG nanoparticles were 11 nm ± 0.06. As a result of the increased permeability and retention (EPR) action, they may expand tumor vasculature (25).

Our results indicated that 400 µg/ml of Ceo-2-XG nanoparticles reduced IC_{50} of 5-FU from 101 to 71 µg/ml, during 72 hours *in vitro* cancer model. Importantly, the synthesized Ceo-2-XG nanoparticles did not show significant toxicity, even at 1000 µg/ml (toxicity rate is less than 50%) except for 72 hours (this means a time-dependent manner).

Apoptosis is the most common kind of programmed cell death which is distinguished by nuclear chromatin condensation, loss of plasma membrane blebbing, DNA breaking and formation of apoptotic bodies (26). Cancer complications may occur at any stage of apoptosis. Downregulation of the *P53* tumor suppressor gene may diminish apoptosis and promote tumor growth (27).

In the present study, we found that cancer cells treated with the 5-FU and Ceo-2-XG nanoparticles demonstrated increased *P53* gene expression, than the 5-FU alone. Bcl2 family proteins are major supervisors of apoptosis (28). Bcl-2 protein inhibits apoptosis. This finding revolutionized cancer pathology since tumorigenesis could be due to unrestricted proliferation and reduced apoptosis. As the main promoter of apoptosis, Bax has been recognized as a talented predictive indicator in cancer (29). Previous studies revealed Bax up-regulation and Bcl-2 downregulation throughout apoptosis in human cancer cells (28). Bcl-2 overexpression in cancer cells has been linked to improve marker diagnosis in colorectal, breast, gastric and glioma malignancies (30).

According to the previous studies, measurement of *BCL-2* gene expression could be used to know treatment response (30). In this work, *BAX* was studied via qRT-PCR assay to evaluate apoptotic pathways after the 5-FU and Ceo-2-XG nanoparticles co-incubation treatment in the Caco-2 cells. Surprisingly, *BAX* gene expression level was much greater in the cancer cells co-incubated with the 5-FU and Ceo-2-XG nanoparticles than the cancer cells treated with the 5-FU alone.

Interestingly, when 5-FU and Ceo-2-XG nanoparticles were co-incubated with cancer cells, *BCL-2* gene expression was considerably reduced in comparison with 5-FU alone. Caspase genes have critical roles in apoptosis and inflammation. As a result, caspases are categorized according to their roles in apoptosis (caspase-3, caspase-6, caspase-7, caspase-8 and caspase-9 in mammals) and inflammation (caspase-1, caspase-4, caspase-5, caspase-12 in humans and caspase-1, caspase-11 and caspase-12 in mice). Caspase-8 and caspase-9 are initiators of apoptosis, whereas caspase-3, caspase-6 and caspase-7 are executioner factors. Executor caspases are turned on by initiator caspases, which then work together to activate several enzymes. DNA fragmentation and membrane blebbing are structural markers of apoptosis in cells (31). In this study, we discovered when 5-FU and Ceo-2-XG nanoparticles were co-incubated with cancer cells, expression of *CASPASE-3*, *CASPASE-8* and *CASPASE-9* genes was much higher than using 5-FU alone.

Our results are the first report to demonstrate that co-incubated 5-FU and Ceo-2-XG nanoparticles induced *BAX*, *P53*, *CASPASE-3*, *CASPASE-8* and *CASPASE-9* mediated apoptosis in Caco-2 cells.

CXCR1/2 and CXCL8 stimulated inflammatory mediators, cancer and metastasis. CXCL8-CXCR1/2 signaling pathway is contributed to the pathophysiology of various illnesses, comprising cancer, asthma and cystic fibrosis. CXCR1/2 and CXCL8 (secreted by cancer cells) interact in the tumour microinvironment, which is detrimental to metastasis. Numerous preclinical studies

indicated that combining CXCR1/2 inhibitors with immunotherapy and chemotherapies might be a potential cancer treatment approach (32).

Previous research has shown that CXCL8 and CXCR2 were overexpressed in CRC tumor tissues (33). *CXCR1*, *CXCR2* and *CXCR8* gene expressions were shown to be increased in metastatic colon cancer cell lines (32). *CXCL1* expression was shown to be greater in the primary colon adenocarcinoma than the normal colon epithelium, according to a review of the literature. *CXCL1* siRNA inhibition reduced proliferation, while increasing apoptosis (34).

Previous research has shown that colon cancer cell lines expressed CXCR2 (35). CXCR2 knock-down reduced cell invasion in the C166 and 4T1 (metastatic murine mammary carcinoma cell lines), while it enhanced doxorubicin and paclitaxel cytotoxicity *in vitro* and *in vivo* mouse models (36, 37). CXCL8 up-regulation has boosted cell proliferation, migration, invasion and resistance to oxaliplatin in HCT116 and Caco-2 cancer cells. CXCL8 over-expression results in larger tumors in xenograft models (38).

In the current work, *CXCR1*, *CXCR2* and *CXCL8* gene expressions were considerably lower in the 5-FU and Ceo-2-XG nanoparticles co-incubated treated cancer cells, than the 5-FU alone. The 5-FU and xanthan gum-based CeO_2 NPsdramatically reduced *CXCR1*, *CXCR2*, and *CXCL8* oncogenes in the Caco-2 cancer cell line compared to the 5-FU alone. As a result, we strongly recommend our working model.

Interestingly, our flow cytometry data revealed that number of dead cells, owing to apoptosis, was twice more in cancer cells co-incubated with the 5-FU and Ceo-2-XG nanoparticles rather than the 5-FU alone. Early apoptotic cells were more than five times higher in cancer cells co-incubated with the 5-FU and Ceo-2-XG nanoparticles than the 5-FU alone. Early apoptotic cells were more than 41 times higher in cancer cells co-incubated with the 5-FU and Ceo-2-XG nanoparticles than the untreated cancer cells in the control group.

Our *in vitro* flow cytometry investigation revealed when the 5-FU and Ceo-2-XG nanoparticles are co-incubated, human malignant colon cancer cell line (Caco-2) is more susceptible to apoptosis than the 5-FU alone. Our light microscopy findings indicated that after 72 hours of co-incubation with the 5-FU and Ceo-2-XG nanoparticles, morphological alterations (many cells with irregularly shaped masses and reduced cell density) was dramatically increased in Caco-2 cancer cells.

To summarize, light microscopy findings was consistent with qRT-PCR results. Findings suggested that co-incubated 5-FU and Ceo-2-XG nanoparticles model is a potent treatment strategy for human colorectal cancer. The co-incubated model revealed a synergistic interaction between 5-FU and CeO_2 NPs derived from xanthan gum.

Conclusion

In the present study, chemotherapeutic activity of the drug 5-FU was enhanced upon its co-incubation with Ceo-2-XG nanoparticles in order to build a novel, less intrusive method against malignant humans colorectal cancer cells (Caco-2). Our *in vitro* cytotoxicity data revealed that lower concentration of 5-FU co-incubated with Ceo-2-XG nanoparticles led to similar activity than free drug (Cayman Thermo Fisher Scientific, USA) alone. Average diameter of Ceo-2-XG nanoparticles was approximately 11 nm. Our results showed that 400 µg/ml nanoparticles significantly reduced IC_{50} of 5-FU from 101 to 71 µg/ml during 72 hours. Amazingly, 5-FU co-incubation with Ceo-2-XG nanoparticles significantly increased apoptosis through *CASPASE-3*, *CASPASE-8*, *CASPASE-9*, *P53* and *BAX* dependent pathways in the Caco-2 cancer cells. In light of these positive findings, it is reasonable to expect that CeO_2 NPs based on 5-FU and xanthan gum will continue to develop into a useful drug delivery system against CRC.

Acknowledgements

This research did not receive any specific grant from any funding agency in the public or commercial. The author declare that they have no conflict of interest.

Authors' Contributions

G.R.M.; Conducted and supervised the study design, data collection and evaluation, drafting and statistical analysis. He was also in charge of overall direction and planning. Z.K; Contributed to conception and design, perfumed data collection and all of the experimental work. A.R.; Synthesized Xanthan Gum-based Cerium Oxide Nanoparticles, approved the final version of this manuscript for submission and contributed to the project as co-supervisor. M.A.K.; Data collection and validation. All authors read and approved the final manuscript.

References

1. Pourmoshir N, Motalleb GH, Vallian S. hsa-miR-423 rs6505162 is associated with the increased risk of breast cancer in isfahan central province of Iran. Cell J. 2020; 22 Suppl 1: 110-116.
2. Sung H, Ferlay J, Siegel RL, Laversanne M, Soerjomataram I, Jemal A, et al. Global cancer statistics 2020: GLOBOCAN estimates of incidence and mortality worldwide for 36 cancers in 185 countries. CA Cancer J Clin. 2021; 71(3): 209-249.
3. Munteanu I, Mastalier B. Genetics of colorectal cancer. J Med Life. 2014; 7(4): 507-511.
4. Pandey S, De Klerk C, Kim J, Kang M, Fosso-Kankeu E. Eco friendly approach for synthesis, characterization and biological activities of milk protein stabilized silver nanoparticles. Polymers (Basel). 2020; 12(6): 1418.
5. Li C, Shi X, Shen Q, Guo C, Hou Z, Zhang J. Hot topics and challenges of regenerative nanoceria in application of antioxidant therapy. J Nanomater. 2018; 2018: 1-12.
6. Elmore S. Apoptosis: a review of programmed cell death. Toxicol Pathol. 2007; 35(4): 495-516.
7. Singh S, Wu S, Varney M, Singh AP, Singh RK. CXCR1 and CXCR2 silencing modulates CXCL8-dependent endothelial cell proliferation, migration and capillary-like structure formation. Microvasc Res. 2011; 82(3): 318-325.
8. Rahdar A, Aliahmad M, Hajinezhad MR, Samani M. Xanthan gum-stabilized nano-ceria: green chemistry based synthesis, characterization, study of biochemical alterations induced by intraperitoneal

doses of nanoparticles in rat. J Mol Struct. 2018; 1173; 166-172.
9. Levit SL, Yang H, Tang C. Rapid self-assembly of polymer nanoparticles for synergistic codelivery of paclitaxel and lapatinib via flash nanoprecipitation. Nanomaterials (Basel). 2020; 10(3): 561.
10. Suzuki R, Kang Y, Li X, Roife D, Zhang R, Fleming JB. Genistein potentiates the antitumor effect of 5-Fluorouracil by inducing apoptosis and autophagy in human pancreatic cancer cells. Anticancer Res. 2014; 34(9): 4685-4692.
11. Sargazi S, Hajinezhad MR, Barani M, Rahdar A, Shahraki S, Karimi P, et al. Synthesis, characterization, toxicity and morphology assessments of newly prepared microemulsion systems for delivery of valproic acid. J Mol Liq. 2021; 338: 116625.
12. Le Berre M, Gerlach JQ, Dziembała I, Kilcoyne M. Calculating half maximal inhibitory concentration (IC50) values from glycomics microarray data using GraphPad Prism. Methods Mol Biol. 2022; 2460: 89-111.
13. Livak KJ, Schmittgen TD. Analysis of relative gene expression data using real-time quantitative PCR and the 2(-delta delta C(T)) method. Methods. 2001; 25(4): 402-408.
14. Koressaar T, Remm M. Enhancements and modifications of primer design program Primer3. Bioinformatics. 2007; 23(10): 1289-1291.
15. Ye J, Coulouris G, Zaretskaya I, Cutcutache I, Rozen S, Madden TL. Primer-BLAST: a tool to design target-specific primers for polymerase chain reaction. BMC Bioinformatics. 2012; 13: 134.
16. Shen YH, Wang LY, Zhang BB, Hu QM, Wang P, He BQ, et al. Ethyl rosmarinate protects high glucose-induced injury in human endothelial cells. Molecules. 2018; 23(12): 3372.
17. Heidarzadeh S, Motalleb GH, Zorriehzahra MJ. Evaluation of tumor regulatory genes and apoptotic pathways in the cytotoxic effect of cytochalasin h on malignant human glioma cell line (U87MG). Cell J. 2019; 21(1): 62-69.
18. Latchman J, Guastella A, Tofthagen C. 5-Fluorouracil toxicity and dihydropyrimidine dehydrogenase enzyme: implications for practice. Clin J Oncol Nurs. 2014; 18(5): 581-585.
19. Gulbake A, Jain A, Jain A, Jain A, Jain SK. Insight to drug delivery aspects for colorectal cancer. World J Gastroenterol. 2016; 22(2): 582-599.
20. Brar B, Ranjan K, Palria A, Kumar R, Ghosh M, Sihag S, et al. Nanotechnology in colorectal cancer for precision diagnosis and therapy. Front Nanosci.2021; 3: 699266.
21. Sisubalan N, Ramkumar VS, Pugazhendhi A, Karthikeyan C, Indira K, Gopinath K, et al. ROS-mediated cytotoxic activity of ZnO and CeO2 nanoparticles synthesized using the Rubia cordifolia L. leaf extract on MG-63 human osteosarcoma cell lines. Environ Sci Pollut Res Int. 2018; 25(11): 10482-10492.
22. Palaniraj A, Jayaraman V. Production, recovery and applications of xanthan gum by Xanthomonas campestris. J Food Eng. 2011; 106(1): 1-12.
23. Stone V, Johnston H, Schins RP. Development of in vitro systems for nanotoxicology: methodological considerations. Crit Rev Toxicol. 2009; 39(7): 613-626.
24. Lee WH, Loo CY, Traini D, Young PM. Inhalation of nanoparticles-based drug for lung cancer treatment: advantages and challenges. Asian J Pharm Sci. 2015; 10: 481-489.
25. Su Y, Hu J, Huang Z, Huang Y, Peng B, Xie N, et al. Paclitaxel-loaded star-shaped copolymer nanoparticles for enhanced malignant melanoma chemotherapy against multidrug resistance. Drug Des Devel Ther. 2017; 11: 659-668.
26. Danial NN, Korsmeyer SJ. Cell death: critical control points. Cell. 2004; 116(2): 205-219.
27. Bauer JH, Helfand SL. New tricks of an old molecule: lifespan regulation by p53. Aging Cell. 2006; 5(5): 437-440.
28. Naseri MH, Mahdavi M, Davoodi J, Tackallou SH, Goudarzvand M, Neishabouri SH. Up regulation of Bax and down regulation of Bcl2 during 3-NC mediated apoptosis in human cancer cells. Cancer Cell Int. 2015; 15: 55.
29. Aali N, Motalleb G. The effect of nicotine on the expressions of the α7 nicotinic receptor gene and Bax and Bcl-2 proteins in the mammary gland epithelial-7 breast cancer cell line and its relationship to drug resistance. Cell Mol Biol Lett. 2015; 20(5): 948-964.
30. Labi V, Erlacher M. How cell death shapes cancer. Cell Death Dis. 2015; 6(3): e1675.
31. McIlwain DR, Berger T, Mak TW. Caspase functions in cell death and disease. Cold Spring Harb Perspect Biol. 2013; 5(4): a008656.
32. Ha H, Debnath B, Neamati N. Role of the CXCL8-CXCR1/2 axis in cancer and inflammatory diseases. Theranostics. 2017; 7(6): 1543-1588.
33. Erreni M, Bianchi P, Laghi L, Mirolo M, Fabbri M, Locati M, et al. Expression of chemokines and chemokine receptors in human colon cancer. Methods Enzymol. 2009; 460: 105-121.
34. Wen Y, Giardina SF, Hamming D, Greenman J, Zachariah E, Bacolod MD, et al. GROalpha is highly expressed in adenocarcinoma of the colon and down-regulates fibulin-1. Clin Cancer Res. 2006; 12(20 Pt 1): 5951-5959.
35. Ogata H, Sekikawa A, Yamagishi H, Ichikawa K, Tomita S, Imura J, et al. GROα promotes invasion of colorectal cancer cells. Oncol Rep. 2010; 24(6): 1479-1486.
36. Sharma B, Nawandar DM, Nannuru KC, Varney ML, Singh RK. Targeting CXCR2 enhances chemotherapeutic response, inhibits mammary tumor growth, angiogenesis, and lung metastasis. Mol Cancer Ther. 2013; 12(5): 799-808.
37. Nannuru KC, Sharma B, Varney ML, Singh RK. Role of chemokine receptor CXCR2 expression in mammary tumor growth, angiogenesis and metastasis. J Carcinog. 2011; 10: 40.
38. Ning Y, Manegold PC, Hong YK, Zhang W, Pohl A, Lurje G, et al. Interleukin-8 is associated with proliferation, migration, angiogenesis and chemosensitivity in vitro and in vivo in colon cancer cell line models. Int J Cancer. 2011; 128(9): 2038-2049.